ADVANCED MATERIALS
www.advmat.de

Combretastatin A4 Nanodrug-Induced MMP9 Amplification Boosts Tumor-Selective Release of Doxorubicin Prodrug

Jian Jiang, Na Shen, Tianyuan Ci, Zhaohui Tang, Zhen Gu,* Gao Li, and Xuesi Chen**

Tumor-associated enzyme-activated prodrugs can potentially improve the selectivity of chemotherapeutics. However, the paucity of tumor-associated enzymes which are essential for prodrug activation usually limits the antitumor potency. A cooperative strategy that utilizes combretastatin A4 nanodrug (CA4-NPs) and matrix metalloproteinase 9 (MMP9)-activated doxorubicin prodrug (MMP9-DOX-NPs) is developed. CA4 is a typical vascular disrupting agent that can selectively disrupt immature tumor blood vessels and exacerbate the tumor hypoxia state. After treatment with CA4-NPs, MMP9 expression can be significantly enhanced by 5.6-fold in treated tumors, which further boosts tumor-selective active drug release of MMP9-DOX-NPs by 3.7-fold in an orthotopic 4T1 mammary adenocarcinoma mouse model. The sequential delivery of CA4-NPs and MMP9-DOX-NPs exhibits enhanced antitumor efficacy with reduced systemic toxicity compared with the noncooperative controls.

Tumor-associated enzyme–activated prodrug (TAEAP) is a class of chemotherapeutics that can be specifically activated within treated tumors where the enzyme is overexpressed and releases its potent naive drug.[1] This strategy is capable of improving the selectivity of chemotherapy and reducing the side effects, thus having received growing attention.[2] The tumor selectivity of TAEAP could be controlled via the structure design of the prodrugs and the type selection of tumor-associated enzymes.[3] Several typical tumor-associated enzymes, such as cathepsin proteases, prostate-specific antigen, and matrix metalloproteinases (MMPs), have been proposed in previous work and proved to be successful in triggering the release of the active compound from TAEAP within tumors.[4] However, one major limitation that could interfere the effectiveness of TAEAPs is the paucity of enzymes which is essential for the prodrug activation within a tumor.[5]

Leverage of the tumor response to cancer therapy is an effective attempt in improving the level of enzymes in tumor sites.[6] There has been report that the chemotherapy of gemcitabine or 5-fluorouracil could increase the levels of cathepsin protease in myeloid-derived suppressor cells.[7] And, radiotherapy has also been confirmed to be efficient in increasing the expression of MMPs in treated tumors.[8] However, traditional chemotherapy lacks selectivity and could not selectively increase the level of enzymes within tumors, while the radiotherapy is usually adopted as a localized therapy and unsuitable for treating disseminated or metastasized tumors.[9]

Vascular disrupting agents (VDAs) could selectively modulate tumor microenvironment by preferentially disrupting immature tumor blood vessels.[10] As a representative low-molecular-weight VDA, combretastatin A4 phosphate (CA4P) could elicit extensive tumor necrosis, while leaving the normal tissues relatively intact.[11] Recently, we developed a combretastatin A4 nanodrug (CA4-NPs) that exhibited higher selectivity to tumor blood vessels than CA4P.[12] In this work, we demonstrated that treatment with CA4-NPs could selectively enhance the expression of MMP9 in the tumor tissues. Because MMP9 could activate the enzyme-activated prodrug of doxorubicin, CA4-NPs could serve as a mediator and cooperator to realize the selective drug release of the MMP9-activated doxorubicin prodrug (**Figure 1**). In this work, we reported that this cooperative delivery system could efficiently amplify the drug release of MMP9-activated doxorubicin prodrug in tumors by 3.7-fold compared with that of noncooperative controls, enhancing the inhibition efficiency of tumor growth in a preclinical treatment with subcutaneous and orthotopic tumor models in mice.

J. Jiang, Dr. N. Shen, Prof. Z. Tang, Prof. G. Li, Prof. X. Chen
Key Laboratory of Polymer Ecomaterials
Jilin Biomedical Polymers Engineering Laboratory
Changchun Institute of Applied Chemistry
Chinese Academy of Sciences
Changchun 130022, P. R. China
E-mail: ztang@ciac.ac.cn; xschen@ciac.ac.cn

J. Jiang, Prof. Z. Tang, Prof. G. Li, Prof. X. Chen
School of Applied Chemistry and Engineering
University of Science and Technology of China
Hefei 230026, P. R. China

Dr. T. Ci, Prof. Z. Gu
Department of Bioengineering
University of California
Los Angeles, CA 90095, USA
E-mail: guzhen@ucla.edu

Dr. T. Ci, Prof. Z. Gu
California NanoSystems Institute (CNSI)
Jonsson Comprehensive Cancer Center
Center for Minimally Invasive Therapeutics
University of California
Los Angeles, CA 90095, USA

The ORCID identification number(s) for the author(s) of this article can be found under https://doi.org/10.1002/adma.201904278.

DOI: 10.1002/adma.201904278

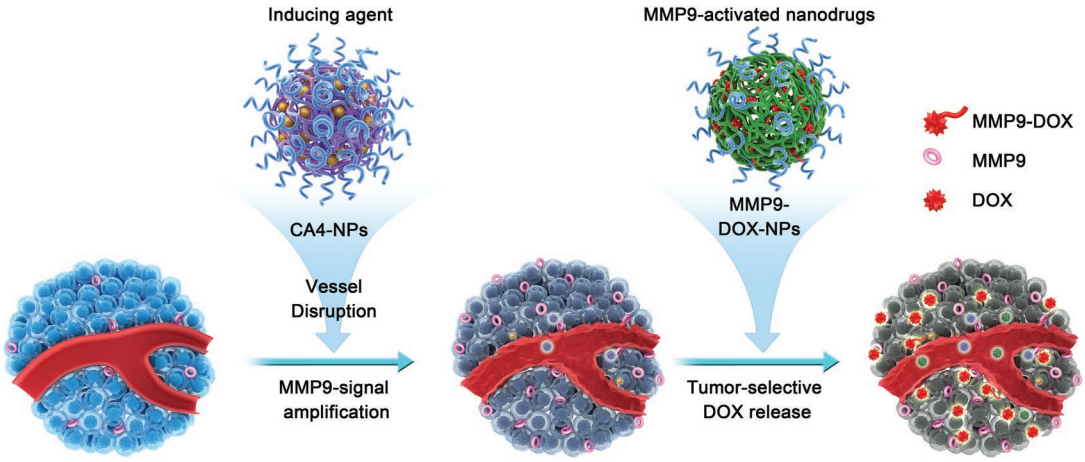

Figure 1. Illustration of cooperative cancer treatment by combining combretastatin A4 nanodrug plus MMP9-activated doxorubicin prodrug nanomedicine. CA4-NPs disrupt tumor vasculature and selectively enhance the expression of MMP9 in the treated tumor, boosting tumor-selective active drug release of MMP9-DOX-NPs.

The MMP9-activated doxorubicin prodrug (Fmoc-GPLGL-DOX, MMP9-DOX) was synthesized by conjugation of doxorubicin to Fmoc-GPLGL (**Figure 2**A). MMP9-DOX was then encapsulated in methoxy poly(ethylene glycol)-*b*-poly(L-glutamic acid-*co*-L-phenylalanine) nanoparticles to yield MMP9-DOX-NPs. Detailed information about the preparation and

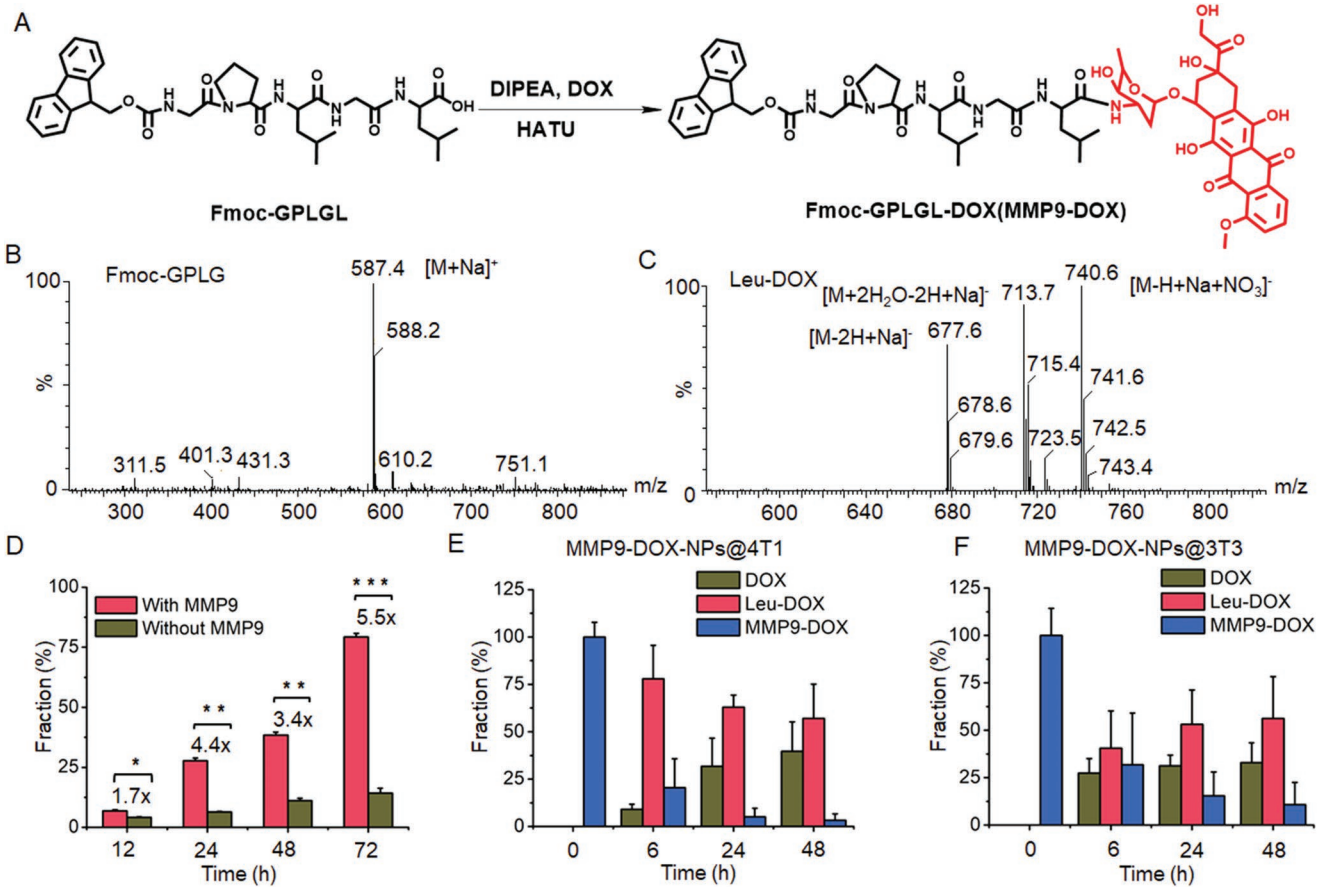

Figure 2. Preparation and characterization of MMP9-DOX-NPs. A) Synthesis of Fmoc-GPLGL-DOX (MMP9-DOX). B) Fmoc-GPLG fragment cleaved by MMP9 from MMP9-DOX, as determined by UPLC-MS. C) The Leu-DOX fragment cleaved by MMP9 from MMP9-DOX, as determined by UPLC-MS. D) Leu-DOX released from MMP9-DOX with or without MMP9 enzyme in vitro ($n = 3$); $^{*}p < 0.05$, $^{**}p < 0.01$, $^{***}p < 0.001$. Amount of Leu-DOX and DOX generated from MMP9-DOX-NPs in culture with E) 4T1 and F) 3T3 cells ($n = 3$). Values represent the fraction of all doxorubicin-containing compounds detected. The results are presented as mean ± standard deviation (SD).

characterization of MMP9-DOX and MMP9-DOX-NPs was described in Figures S1 and S2 (Supporting Information).

To evaluate the MMP9 sensitivity of MMP9-DOX, the enzymatic cleavage of MMP9-DOX was investigated. As shown in Figure 2B,C, the main fragments cleaved by MMP9 were Fmoc-GPLG ($[M + Na]^+ = 587.4$) and Leu-DOX ($[M - 2H + Na]^- = 677.6$, $[M + 2H_2O - 2H + Na]^- = 713.7$, and $[M - H + Na + NO_3]^- = 740.6$) identified by ultra performance liquid chromatography–mass spectrometry (UPLC-MS) (Figure S3, Supporting Information). This indicated that the main cleavage site was between the Gly and Leu amino acid residues in the Fmoc-GPLGL-DOX. And, Leu-DOX could be released from MMP9-DOX in the presence of MMP9. The triggered drug release profile from MMP9-DOX was shown in Figure 2D. The amounts of released Leu-DOX in the presence of MMP9 were 1.7-fold, 4.4-fold, 3.4-fold, and 5.5-fold compared with that in the absence of MMP9 at 12, 24, 48, and 72 h, respectively. These data further confirmed that the prodrug of MMP9-DOX was sensitive to MMP9.

The MMP9 sensitivity of MMP9-DOX and MMP9-DOX-NPs was also investigated by evaluation of their intracellular metabolism. Relative protein content and messenger ribonucleic acid (mRNA) expression of MMP9 were determined in 12 cell lines. As evaluated by gelatin zymography and reverse transcriptase-polymerase chain reaction assays (Figure S4, Supporting Information), the 4T1 cell line expressed high level of MMP9, while the 3T3 cell line expressed low level of MMP9. The level of Leu-DOX cleaved from MMP9-DOX and MMP9-DOX-NPs in 4T1 cells was higher than that in 3T3 cells (Figure 2E,F and Figure S5 (Supporting Information)). The molar ratios of [Leu-DOX]/[MMP9-DOX] in the MMP9-DOX@4T1 group were 3.6, 16.1, and 46.7 at 6, 24, and 48 h, respectively. The molar ratios of [Leu-DOX]/[MMP9-DOX] in the MMP9-DOX-NPs@4T1 group were 4.3, 18.6, and 30.2 at 6, 24, and 48 h, respectively. By contrast, the molar ratios of [Leu-DOX]/[MMP9-DOX] in the MMP9-DOX@3T3 group were significantly decreased to 1.6, 3.1, and 7.2 at 6, 24, and 48 h, respectively, and 2.1, 5.4, and 8.2 in the MMP9-DOX-NPs@3T3 group at 6, 24, and 48 h, respectively (Table S1, Supporting Information). These results indicated that MMP9-DOX and MMP9-DOX-NPs could be cleaved to Leu-DOX more efficiently in cells with high MMP9 level than those with low MMP9 level. Meanwhile, considering that aminopeptidases are widely distributed throughout animal cells, Leu-DOX would gradually convert into free DOX and prohibit the proliferation of cancer cells.[13] In fact, all formulations, including free DOX, MMP9-DOX, and MMP9-DOX-NPs, showed time- and concentration-dependent suppression of 4T1 tumor cell proliferation (Figure S6, Supporting Information). Free DOX showed the strongest antitumor efficiency with the lowest half maximal inhibitory concentration (IC_{50}) values compared with other two groups, while MMP9-DOX-NPs were the least potent in tumor inhibition in vitro (IC_{50}(free DOX) < IC_{50}(MMP9-DOX) < IC_{50}(MMP9-DOX-NPs) (Table S2, Supporting Information). This could be attributed to the reason that MMP9-DOX was a prodrug of free DOX, and MMP9-DOX-NPs was a sustained-release formulation of MMP9-DOX.

The MMP9 signal amplification induced by CA4-NPs was then investigated in BALB/c mice bearing 4T1 mammary carcinoma. The CA4-NPs were prepared by the Yamaguchi reaction of CA4 with poly(L-glutamic acid)-*graft*-methoxy poly(ethylene glycol) (Figure S7, Supporting Information). Immunofluorescence staining assay indicated that CA4-NPs treatment significantly increased the expression of MMP9 in tumor tissues (**Figure 3**A). The relative protein expression of MMP9 in the CA4-NPs group was 5.6-fold of that in the phosphate-buffered saline (PBS) group 48 h after intravenous injection (Figure 3B). The level of MMP9 in the tumor tissues was also measured by Western blot analysis (Figure 3C,D) and gelatin zymography (Figure S8, Supporting Information). A significant increase in MMP9 expression was observed in the CA4-NPs group compared with the PBS group. Furthermore, we compared the level of MMP9 in normal organs of CA4-NPs and PBS groups. The normal organs (heart, liver, spleen, lung, and kidney) of the CA4-NPs group exhibited similar level of MMP9 as that of PBS group at 48 h postinjection (Figure 3E and Figure S9 (Supporting Information)). These results provided evidence that the MMP9 signal amplification induced by CA4-NPs selectively occurred inside the tumors rather than other normal organs.

We further analyzed the factors contributing to MMP9 signal amplification in the tumors treated with CA4-NPs. Considering that CA4-NPs treatment could lead to severe hypoxic microenvironment in solid tumors,[14] and the expression of MMP9 in tumors could be regulated by hypoxia.[15] We investigated vascular density and hypoxia state in tumor tissues after CA4-NPs treatment. Immunofluorescence imaging assay of CD31 revealed that the blood vessel density of CA4-NPs group was lower than that in PBS group (Figure S10A, Supporting Information). Additionally, the expression of HIF-1α of CA4-NPs group was higher than that in PBS group (Figure S10B, Supporting Information). These indicated that CA4-NPs could disrupt tumor vessels and induce severe hypoxia in tumor tissues. We further compared the level of MMP9 in 4T1 tumor cells under normoxic (20% oxygen) and simulated hypoxic (1% oxygen) conditions. Both Western blot analysis and gelatin zymography assays revealed that the expression of MMP9 increased significantly under hypoxic condition whether in the PBS group or in the CA4-NPs group. The expression of MMP9 under hypoxic condition was 1.3-fold–1.5-fold of that under normoxic condition (Figure 3F,G and Figure S11 (Supporting Information)). These results revealed that CA4-NPs-induced hypoxia was the key factor for MMP9 signal amplification in tumors.

To investigate the influence of treatment with CA4-NPs on the active drug release of MMP9-DOX-NPs in vivo, the tissue distribution of free DOX was studied in orthotopic 4T1 tumor-bearing mice because of Leu-DOX could be cleaved to free DOX by widespread aminopeptidases.[16] Female BALB/c mice bearing tumors (≈150 mm^3) were randomly divided into two groups: MMP9-DOX-NPs (5 mg kg^{-1} on DOX basis) and CA4-NPs (30 mg kg^{-1} on CA4 basis) + MMP9-DOX-NPs (5 mg kg^{-1} on DOX basis). At 48 h postinjection, the tumor and normal organs were separated for quantification of free DOX. Free DOX concentration in the 4T1 tumors was significantly higher (2.7-fold, $p < 0.001$) in the CA4-NPs (30 mg kg^{-1} on CA4 basis) + MMP9-DOX-NPs (5 mg kg^{-1} on DOX basis) group compared with the MMP9-DOX-NPs (5 mg kg^{-1} on DOX basis) group (**Figure 4**A), while no significant difference between the two groups was observed in normal organs, such as the heart, liver, spleen, lung, and kidney (Figure 4B). These results demonstrated that leveraging the vascular-disrupting effect of

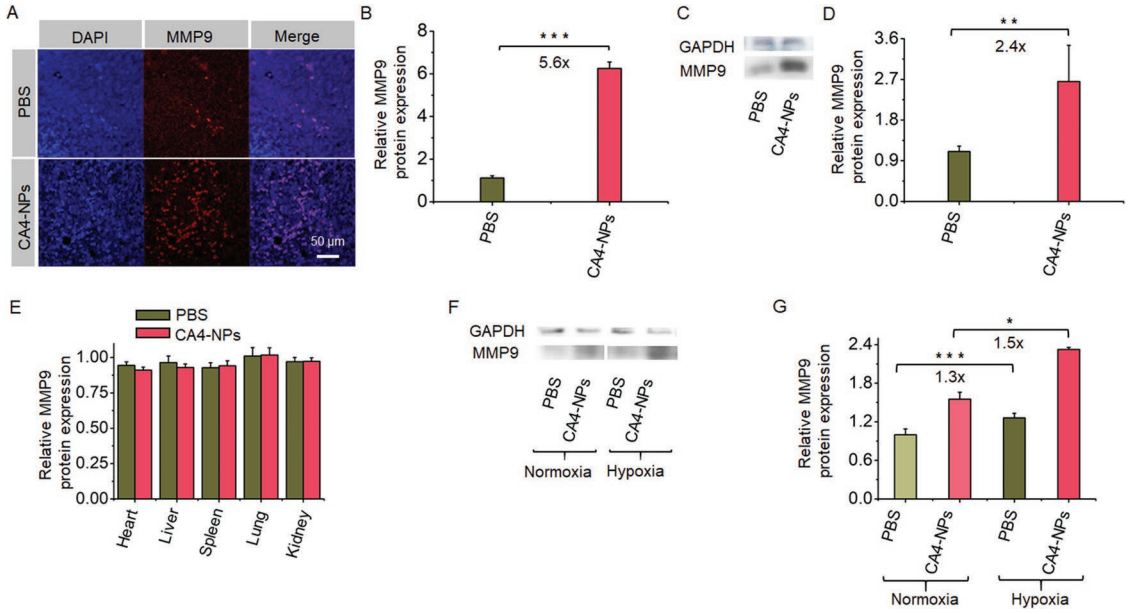

Figure 3. CA4-NPs-induced MMP9 signal amplification. The level of MMP9 at 48 h in 4T1 tumors (≈150 mm^3) treated with PBS or CA4-NPs (30 mg kg^{-1} on CA4 basis). A) Immunofluorescence staining assay for MMP9 of 4T1 tumor tissues, the scale bar represents 50 μm. B) Quantitative analysis of the expression of MMP9 in tumor tissues measured by immunofluorescence staining assay ($n = 3$). C) MMP9 level in the tumor tissues as demonstrated by Western blot analysis. D) The quantification analysis of the expression of MMP9 in tumor tissues measured by Western blot ($n = 3$). E) Quantitative analysis of MMP9 level in normal organ tissues of the two groups ($n = 3$). In (B), (D), (E), MMP9 level in the tumor tissues of PBS group represent the reference value. F) MMP9 level in 4T1 cells cultured in different conditions for 48 h. G) The quantification analysis of the expression of MMP9 in 4T1 cells measured by Western blot ($n = 3$). MMP9 level was calculated relative to the reference value, which was represented by MMP9 level in the PBS group in normal oxygen condition. CA4-NPs dose: 5 ng mL^{-1} on CA4 basis. *$p < 0.05$, **$p < 0.01$, ***$p < 0.001$. The results are presented as mean ± standard deviation.

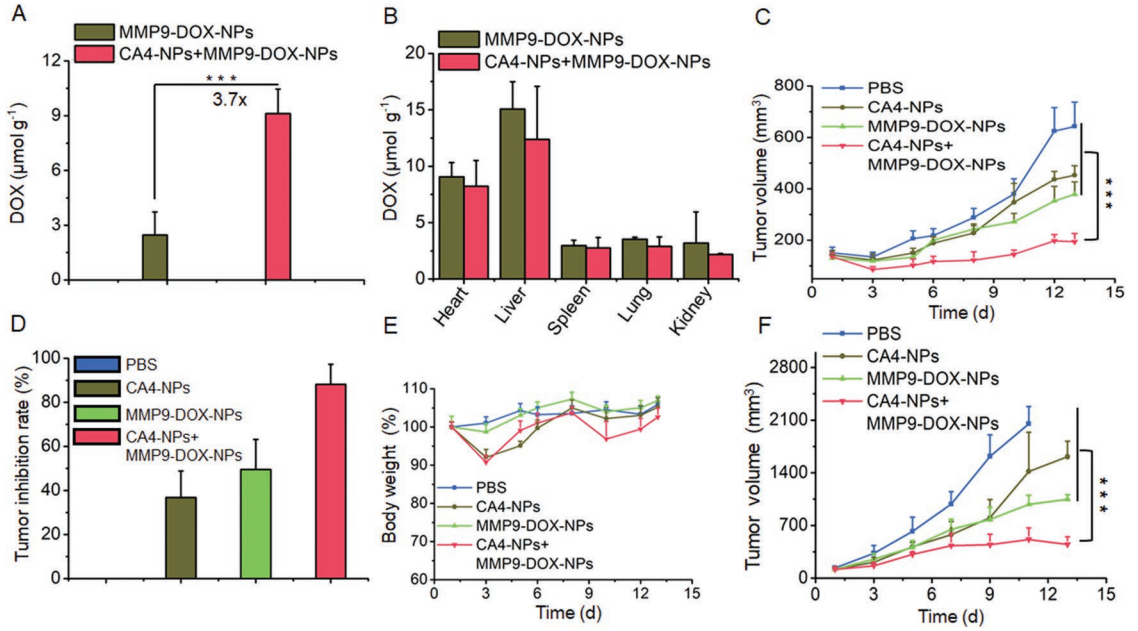

Figure 4. Free doxorubicin distribution in tissues and in vivo tumor inhibition following treatment with a combination of CA4-NPs and MMP9-DOX-NPs. A) Free doxorubicin distribution in tumor tissues ($n = 6$ mice per group). B) Free doxorubicin distribution in normal organ tissues. C) Tumor volume change in orthotopic 4T1 tumor model during treatment ($n = 5$ mice per group). D) Tumor inhibition rate in 4T1 tumor model. E) Change in body weight in 4T1 tumor model. F) Tumor volume change in subcutaneous C26 tumor model during treatment ($n = 6$ mice per group). Doses of DOX and CA4 basis were 5 and 30 mg kg^{-1}, respectively. Data represent means ± SD, statistical analysis by one-way analysis of variance (ANOVA) and Tukey's test: *$p < 0.05$; **$p < 0.01$; ***$p < 0.001$. The results are presented as mean ± standard deviation.

CA4-NPs could significantly enhance tumor selective release of MMP9-activated doxorubicin prodrug nanomedicine, consistent with previous findings that CA4-NPs treatment–induced MMP9 signal amplification occurred selectively inside tumors.

Tumor-selective MMP9 signal amplification through treatment with CA4-NPs provided a rationale for studying the therapeutic efficacy of the combination of CA4-NPs plus MMP9-DOX-NPs in an orthotopic 4T1 mammary adenocarcinoma model. The more MMP9-DOX-NPs targetingly released in tumor tissues, the more Leu-DOX released from MMP9-DOX by MMP9 and more DOX released in tumor tissues by aminopeptidases for tumor cells inhibition. Female BALB/c mice bearing tumors (≈150 mm^3) were randomly divided into four groups: PBS, CA4-NPs (30 mg kg^{-1} on CA4 basis), MMP9-DOX-NPs (5 mg kg^{-1} on DOX basis), and CA4-NPs (30 mg kg^{-1} on CA4 basis) + MMP9-DOX-NPs (5 mg kg^{-1} on DOX basis). The treatment regimen was shown in Figure S12 (Supporting Information). Tumor volume and body weight of the mice were monitored for 13 days. Monotherapies with either CA4-NPs or MMP9-DOX-NPs demonstrated a moderate effect of inhibition of tumor growth. Mean tumor volumes were 452.5 ± 37.4 and 378.1 ± 48.3 mm^3, and tumor inhibition rates were 36.8% and 49.5% for the CA4-NPs and MMP9-DOX-NPs monotherapy groups, respectively. Consistent with the proposed scenario, combination therapy with CA4-NPs and MMP9-DOX-NPs suppressed tumor growth more strongly compared with either monotherapy. Mean tumor size in the CA4-NPs + MMP9-DOX-NPs group at the end point was 193.7 ± 32.2 mm^3 with a tumor inhibition rate of 88.2%, a 1.8-fold increase compared to the MMP9-DOX-NPs group (Figure 4C,D and Figure S13 (Supporting Information)). The antitumor efficiency was also evaluated by Q value method.[17] The Q value was 1.29 for the CA4-NPs + MMP9-DOX-NPs group, indicating a synergistic interaction of the system. Systemic toxicity was evaluated by assessment of body weight in the treated mice (Figure 4E). Compared with the PBS group, no significant body weight loss was observed in the MMP9-DOX-NPs group. In the CA4-NPs and CA4-NPs + MMP9-DOX-NPs groups, body weight decreased during the early time points (≈9%) but gradually recovered after 7 days. These results revealed that combination treatment with CA4-NPs + MMP9-DOX-NPs exhibited significantly enhanced antitumor efficacy with minimal systemic toxicity compared with noncooperative controls.

To further evaluate the therapeutic effects and systemic toxicity of the treatment, excised tumors and normal organs were stained with hematoxylin and eosin (H&E). As shown in Figure S14 (Supporting Information), a larger number of dead cells was observed in the CA4-NPs + MMP9-DOX-NPs group compared with the other groups, where cells were characterized by hypereosinophilic cytoplasm with small, fragmented nuclei. CA4-NPs or MMP9-DOX-NPs monotherapy displayed a similar antitumor effect, although weaker than the combination therapy. No unusual pathological abnormalities were observed in the H&E-stained normal organs, in any group. These results revealed that the sequential treatment with CA4-NPs and MMP9-DOX-NPs strongly inhibited tumor growth without significant cytotoxicity to normal organs. Hematological analyses were performed to study the biocompatibility and hematological toxicity of the cooperative group on healthy Kunming mice and 4T1-bearing Balb/c mice (tumor volume ≈ 150 mm^3) after 48 h intravenous injection of different formulations. As shown in Figures S15 and S16 (Supporting Information), there were no significant difference in all nine hematological parameters between the cooperative group and PBS group/normal group. All these results indicated the high therapeutic effects with limited systemic toxicity of the cooperative group.

In addition to evaluation using an orthotopic 4T1 mammary adenocarcinoma model, we also evaluated the cooperative strategy on subcutaneous C26 colon tumor-bearing BALB/c mice, where similar results were obtained. The treatment regimen was same as shown in Figure S12 (Supporting Information). Tumor growth was significantly inhibited in the CA4-NPs + MMP9-DOX-NPs group compared with the other groups ($P < 0.001$) with Q value of 1.15 (Figure 4F). While, there was no significant difference in animal body weight among the CA4-NPs, MMP9-DOX-NPs or CA4-NPs + MMP9-DOX-NPs groups (Figure S17, Supporting Information). Collectively, these results suggested that the cooperative strategy of CA4-NPs + MMP9-DOX-NPs had potential for the treatment of various types of cancer.

In summary, we developed a cooperative strategy leveraging sequential delivery of CA4-NPs and MMP9-DOX-NPs to enhance tumor-selective drug release in cancer therapy. We demonstrated that CA4-NPs-induced MMP9 signal amplification boosted tumor-selective drug release of MMP9-DOX-NPs by 3.7-fold ($p < 0.001$). The combination of CA4-NPs + MMP9-DOX-NPs exhibited superior anticancer efficacy compared with monotherapy, highlighting the importance of tumor-selective MMP9 signal amplification of the MMP9-activated prodrug therapy. This cooperative strategy could be leveraged for development of next generation tumor-associated enzyme–activated prodrug systems with reduced toxicity. Future work will focus on the in-depth characterization of the combination of CA4-NPs + MMP9-DOX-NPs, including pharmacokinetics and host immunoresponse. Combination with immunotherapy will also be considered to further improve anticancer efficacy.

Supporting Information

Supporting Information is available from the Wiley Online Library or from the author.

Acknowledgements

J.J. and N.S. contributed equally to this work. This work was financially supported by the National Natural Science Foundation of China (Grant Nos. 51503202, 51673189, 51873206, 51833010, and 51520105004), the Ministry of Science and Technology of China (Grant Nos. 2016YFC1100701 and 2018ZX09711003-012), the Jilin Province (Grant No. 20190103033JH), and the UCLA start-up package to Z.G. All animals in this study were handled under protocols approved by the Institutional Animal Care and Use Committee of Jilin University. All efforts were made to minimize suffering.

Conflict of Interest

The authors declare no conflict of interest.

Keywords

combination delivery, doxorubicin prodrug, drug delivery, matrix metalloproteinases, nanomedicine

Received: July 4, 2019
Revised: August 27, 2019
Published online: September 24, 2019

[1] a) M. H. Lee, A. Sharma, M. J. Chang, J. Lee, S. Son, J. L. Sessler, C. Kang, J. S. Kim, *Chem. Soc. Rev.* **2018**, *47*, 28; b) Q. Yao, F. Lin, X. Fan, Y. Wang, Y. Liu, Z. Liu, X. Jiang, P. R. Chen, Y. Gao, *Nat. Commun.* **2018**, *9*, 5032; c) Y. Lu, A. A. Aimetti, R. Langer, Z. Gu, *Nat. Rev. Mater.* **2017**, *2*, 16075.

[2] a) R. Mahato, W. Tai, K. Cheng, *Adv. Drug Delivery Rev.* **2011**, *63*, 659; b) J. Vandooren, G. Opdenakker, P. M. Loadman, D. R. Edwards, *Adv. Drug Delivery Rev.* **2016**, *97*, 144; c) M. Xiao, W. Sun, J. Fan, J. Cao, Y. Li, K. Shao, M. Li, X. Li, Y. Kang, W. Zhang, S. Long, J. Du, X. Peng, *Adv. Funct. Mater.* **2018**, *28*, 1805128; d) T. Jiang, W. Sun, Q. Zhu, N. A. Burns, S. A. Khan, R. Mo, Z. Gu, *Adv. Mater.* **2015**, *27*, 1021; e) Q. Zhou, S. Shao, J. Wang, C. Xu, J. Xiang, Y. Piao, Z. Zhou, Q. Yu, J. Tang, X. Liu, Z. Gan, R. Mo, Z. Gu, Y. Shen, *Nat. Nanotechnol.* **2019**, *14*, 799.

[3] a) A. P. Blum, J. K. Kammeyer, A. M. Rush, C. E. Callmann, M. E. Hahn, N. C. Gianneschi, *J. Am. Chem. Soc.* **2015**, *137*, 2140; b) S. Mura, J. Nicolas, P. Couvreur, *Nat. Mater.* **2013**, *12*, 991; c) R. Mooney, A. A. Majid, J. Batalla, A. J. Annala, K. S. Aboody, *Adv. Drug Delivery Rev.* **2017**, *118*, 35; d) J. Mu, J. Lin, P. Huang, X. Y. Chen, *Chem. Soc. Rev.* **2018**, *47*, 5554.

[4] a) D. Dheer, J. Nicolas, R. Shankar, *Adv. Drug Delivery Rev.* **2019**, https://doi.org/10.1016/j.addr.2019.01.010; b) R. E. Vandenbroucke, C. Libert, *Nat. Rev. Drug Discovery* **2014**, *13*, 904; c) K. Kessenbrock, V. Plaks, Z. Werb, *Cell* **2010**, *141*, 52; d) O. C. Olson, J. A. Joyce, *Nat. Rev. Cancer* **2015**, *15*, 712; e) T. Wuestemann, U. Haberkorn, J. Babich, W. Mier, *Med. Res. Rev.* **2019**, *39*, 40; f) M. K. Shim, J. Park, H. Y. Yoon, S. Lee, W. Um, J.-H. Kim, S.-W. Kang, J.-W. Seo, S.-W. Hyun, J. H. Park, Y. Byun, I. C. Kwon, K. Kim, *J. Controlled Release* **2019**, *294*, 376.

[5] a) K. S. Aboody, J. Najbauer, M. Z. Metz, M. D'Apuzzo, M. Gutova, A. J. Annala, T. W. Synold, L. A. Couture, S. Blanchard, R. A. Moats, E. Garcia, S. Aramburo, V. V. Valenzuela, R. T. Frank, M. E. Barish, C. E. Brown, S. U. Kim, B. Badie, J. Portnow, *Sci. Transl. Med.* **2013**, *5*, 184ra59; b) G. von Maltzahn, J.-H. Park, K. Y. Lin, N. Singh, C. Schwoeppe, R. Mesters, W. E. Berdel, E. Ruoslahti, M. J. Sailor, S. N. Bhatia, *Nat. Mater.* **2011**, *10*, 545; c) G. G. Dias, A. King, F. de Moliner, M. Vendrell, E. N. da Silva Junior, *Chem. Soc. Rev.* **2018**, *47*, 12; d) J. Du, L. A. Lane, S. Nie, *J. Controlled Release* **2015**, *219*, 205.

[6] a) K. Y. Lin, E. J. Kwon, J. H. Lo, S. N. Bhatia, *Nano Today* **2014**, *9*, 550; b) W. J. Sun, Q. Y. Hu, W. Y. Ji, G. Wright, Z. Gu, *Physiol. Rev.* **2017**, *97*, 189.

[7] M. Bruchard, G. Mignot, V. Derangere, F. Chalmin, A. Chevriaux, F. Vegran, W. Boireau, B. Simon, B. Ryffel, J. L. Connat, J. Kanellopoulos, F. Martin, C. Rebe, L. Apetoh, F. Ghiringhelli, *Nat. Med.* **2013**, *19*, 57.

[8] a) E. Fernstrom, K. Minta, U. Andreasson, A. Sandelius, P. Wasling, A. Brinkmalm, K. Hoglund, K. Blennow, J. Nyman, H. Zetterberg, M. Kalm, *J. Intern. Med.* **2018**, *284*, 211; b) G. O. Ahn, J. M. Brown, *Cancer Cell* **2008**, *13*, 193.

[9] a) L. Gandola, M. Massimino, G. Cefalo, C. Solero, F. Spreafico, E. Pecori, D. Riva, P. Collini, E. Pignoli, F. Giangaspero, R. Luksch, S. Berretta, G. Poggi, V. Biassoni, A. Ferrari, B. Pollo, C. Favre, I. Sardi, M. Terenziani, F. Fossati-Bellani, *J. Clin. Oncol.* **2009**, *27*, 566; b) H. E. Barker, J. T. E. Paget, A. A. Khan, K. J. Harrington, *Nat. Rev. Cancer* **2015**, *15*, 409; c) R. R. Weichselbaum, H. Liang, L. Deng, Y.-X. Fu, *Nat. Rev. Clin. Oncol.* **2017**, *14*, 365.

[10] a) S. Sharma, A. P. Mann, T. Molder, V. R. Kotamraju, R. Mattrey, T. Teesalu, E. Ruoslahti, *J. Controlled Release* **2017**, *268*, 49; b) S. Lv, Z. Tang, W. Song, D. Zhang, M. Li, H. Liu, J. Cheng, W. Zhong, X. Chen, *Small* **2017**, *13*. 1600954; c) G. M. Tozer, C. Kanthou, B. C. Baguley, *Nat. Rev. Cancer* **2005**, *5*, 423.

[11] a) W. Song, Z. Tang, D. Zhang, H. Yu, X. Chen, *Small* **2015**, *11*, 3755; b) W. Song, Z. Tang, D. Zhang, M. Li, J. Gu, X. Chen, *Chem. Sci.* **2016**, *7*, 728.

[12] T. Liu, D. Zhang, W. Song, Z. Tang, J. Zhu, Z. Ma, X. Wang, X. Chen, T. Tong, *Acta Biomater.* **2017**, *53*, 179.

[13] K. Gu, Y. Liu, Z. Guo, C. Lian, C. Yan, P. Shi, H. Tian, W.-H. Zhu, *ACS Appl. Mater. Interfaces* **2016**, *8*, 26622.

[14] S. Yang, Z. Tang, C. Hu, D. Zhang, N. Shen, H. Yu, X. Chen, *Adv. Mater.* **2019**, *31*, 1805955.

[15] S. Wang, Y. Yan, Z. Cheng, Y. Hu, T. Liu, *Cell Death Discovery* **2018**, *4*, 26.

[16] a) X. Zhang, X. Li, Q. You, X. Zhang, *Eur. J. Med. Chem.* **2017**, *139*, 542; b) V. Dubois, M. Nieder, F. Collot, A. Negrouk, T. T. Nguyen, S. Gangwar, B. Reitz, R. Wattiez, L. Dasnois, A. Trouet, *Eur. J. Cancer* **2006**, *42*, 3049.

[17] P. Hang, Z. W. Liu, G. G. Zhang, Y. S. Xiao, H. Xu, J. L. Wang, *J. Pract. Med.* **2014**, *5*, 738.

